Natural Resources Canada | Ressources naturelles Canada

GEOLOGICAL SURVEY OF CANADA
OPEN FILE 7874

DInSAR interannual seasonal surface displacement in permafrost terrain, Iqaluit, Nunavut

A.-M. LeBlanc, N. Short, V. Mathon-Dufour, and J. Chartrand

2015

Canada

GEOLOGICAL SURVEY OF CANADA
OPEN FILE 7874

DInSAR interannual seasonal surface displacement in permafrost terrain, Iqaluit, Nunavut

A.-M. LeBlanc[1], N. Short[2], V. Mathon-Dufour[3], and J. Chartrand[1]

[1]Geological Survey of Canada, Natural Resources Canada, Ottawa, Ontario
[2] Canada Centre for Mapping and Earth Observation, Natural Resources Canada, Ottawa, Ontario
[3]Centre d'études nordiques, Université Laval, Québec, Quebec

2015

doi:10.4095/297406

This publication is available for free download through GEOSCAN (http://geoscan.rncan.gc.ca/).

Recommended citation
LeBlanc, A.-M., Short, N., Mathon-Dufour, V., and Chartrand, J., 2015. DInSAR interannual seasonal surface displacement in permafrost terrain, Iqaluit, Nunavut; Geological Survey of Canada, Open File 7874, 1 .zip file. doi:10.4095/297406

Publications in this series have not been edited; they are released as submitted by the author.

SUMMARY

Monitoring permafrost dynamics over large areas is challenging. In recent years, interest in the use of Interferometric Synthetic Aperture Radar (InSAR) as a source of surface displacement information for permafrost environments has increased considerably. Among the available InSAR methods, conventional differential InSAR (DInSAR) makes it possible to detect very small ground surface movement, on the order of centimetres, for every pixel over large areas, providing a way to assess active layer and permafrost dynamics. In order to expand existing knowledge and guide potential applications of DInSAR, three consecutive years of seasonal surface displacement in Iqaluit, Nunavut, were analysed along with surficial units, permafrost and climatic data, and compared for built and natural environments. RADARSAT-2 spotlight scenes with a resolution of approximately 1 m were used to create maps of seasonal ground surface displacement. Results show that surficial geology and ground ice are essential information to interpret DInSAR results: low displacement is associated with bedrock and coarse sediments, while finer sediments, more likely to be ice-rich, show higher values of displacement. Other factors such as water at the surface and mapping scale of surficial deposits, can explain some displacement patterns. One DInSAR season could be used to identify difficult terrain for construction. However, displacement values for a given area can vary from one year to the next due to annual climatic conditions. Therefore, more than one season helps to differentiate between different causes of displacement. For a given surficial geology unit, displacements were generally lower in built areas than in the natural environment due to granular fill or pads and construction methods. Findings from this study are useful to guide DInSAR applications especially for infrastructure management and planning.

Table of Contents

Table of Figures

1 INTRODUCTION

Monitoring permafrost changes and dynamics over large areas is challenging. Ground-based techniques are generally used to assess permafrost properties, active layer thickness, and thaw settlement. Relations between these properties and surficial geology could then be used to interpolate point information over large areas. In recent years, interest in the use of Interferometric Synthetic Aperture Radar (InSAR) as a surface displacement assessment tool for permafrost environments has increased considerably. Among the available InSAR methods, conventional differential InSAR (DInSAR) makes it possible to detect very small ground surface movement, on the order of centimetres, for every pixel over large areas, providing a way to assess active layer and permafrost dynamics (Short et al., 2011).

As part of the Land-Based Infrastructure project within the Geological Survey of Canada (GSC) Climate Change Geoscience Program and the Northern Development and Remote Sensing Science initiative (Canada Centre for Mapping and Earth Observation (CCMEO)), DInSAR data were acquired over consecutive summers (2011 to 2013) for the Iqaluit area, Nunavut. Specific objectives of this activity were to develop and qualitatively/quantitatively validate DInSAR products and assess their usefulness in supporting decision-making for existing or new infrastructure.

A map of DInSAR seasonal surface displacement for Iqaluit during the summer 2011 was previously released as a geotiff format (Short et al., 2012a). Results were briefly examined along with surficial geology and field observations such as near-surface soil moisture and seasonal displacement using thaw tubes (Nixon and Taylor, 1994). However, correlation with surficial geology (Allard et al. 2012) was only assessed qualitatively. Quantitatively, validation with surficial geology was published only for the Iqaluit airport area using the seasonal surface displacement during the summer 2012 (Short et al., 2014). Quantitative and qualitative validations with observed displacements (thaw tubes) and with geophysical characteristics (airport area) for the summer 2012 were also shown by Short et al. (2014).

The objectives of this open file are to 1) provide maps of DInSAR data in geotiff format for years 2012 and 2013, 2) compare the interannual (2011 to 2013) DInSAR seasonal displacement, 3) assess quantitatively the DInSAR seasonal displacement according to surficial geology, and 4) compare the DInSAR seasonal displacement in built and natural environments. The general purpose of this open file is to expand our previous knowledge in order to guide potential applications of DInSAR.

2 STUDY SITE

Iqaluit is located on southeastern Baffin Island at the head of Frobisher Bay (63°45'N, 68°33'W), in a zone of continuous permafrost (Figure 1). Local elevation ranges from 15 to 125 m asl. The old neighbourhoods of the city and the airport are built on flat terrain surrounded by hills and rocky plateaus of the Precambrian Shield (St-Onge et al., 2006) whereas more recent neighbourhoods tend to be located on rocky hill slopes and plateaus. Built areas are often surrounded by disturbed terrain. All the main roads, built on embankment material, are paved,

while buildings rest on piles, fill material or a combination of the two (Figure 2). The tundra vegetation is low growing and generally continuous, except on exposed bedrock outcrops. The dominant vegetation is composed of willow and heath, with extensive areas of grasses, sedges and moss, dependent upon moisture conditions (Short & Jacobs, 1982).

Mean monthly air temperatures for the 1981-2010 climate normals range from 8.2 °C in July to -27.5 °C in February, with an annual mean of -9.3 °C, and with annual precipitation of 404 mm, of which 49% occurred as rain (Environment Canada: http//climate.weather.gc.ca). The permafrost temperature is approximately -5.4 ºC at a depth of 10 m, with an active layer thickness (ALT) of 1.35 m in natural ground and ~2.5 m under paved infrastructure (Mathon-Dufour et al., 2015).

3 DATA

3.1 RADARSAT-2 data

RADARSAT-2 data acquired over Iqaluit were used for the DInSAR analysis. RADARSAT-2 is a C-band SAR satellite launched in December 2007. It operates with a SAR wavelength of 5.6 cm, a repeat orbit of 24 days and offers a variety of acquisition modes. For the Iqaluit area, data were acquired for each year in spotlight mode, with ~1 m resolution, HH polarization, descending orbit, right looking and an incidence angle of 45°. Acquisition dates for each year are shown in Table 1.

Table 1: RADARSAT-2 acquisition dates

	2011	2012	2013
Acquisition dates		May 23	
	June 22	June 15	June 11
	July 16	July 10	July 5
	August 9	August 3	July 29
	September 2	August 27	August 22
	September 26	September 20	September 15

3.2 Surficial geology

The original surficial geology map for the area of Iqaluit was done by Allard et al. (2012) (Figure 3). In old built areas and under the airport infrastructure, the surficial geology units are dominated by glaciomarine (GMd) deposits and nearshore (Mn) sediments. Precambrian bedrock with partial and uneven till cover (till blanket (Tb) and till veneer (Tv)) are found under newly built areas on hilly terrain and plateaus. Some glaciofluvial deposits (GFp) also extend under newly built areas as well as in the northern portions of the runway and the main industrial subdivision. Alluvial floodplain (Ap) and terraced (At) sediments are found along current and old river and stream channels such as the Sylvia Grinnell River and Carney Creek. Patches of

lacustrine sediments have been mapped in more detail for the Iqaluit airport area and are mostly found interspersed with the glaciomarine, nearshore and glaciofluvial deposits.

For the Iqaluit airport area, an updated version of the surficial geology is presented in Mathon-Dufour et al. (2015), which includes the addition of lacustrine sediments within the Iqaluit airport area and an update of the marine limit (including the corresponding boundary between the glaciomarine and glaciofluvial deposits). In this report, the updated version was used for the statistical analysis of seasonal displacement and is shown in Figure 3.

3.3 Climatic data

Climatic data recorded at the Environment Canada weather station AWOS (63°75'N, 68°55'W, elevation 33.5 m) are summarised in Table 2 for summers 2011, 2012, and 2013. The data are given for the summer months (JJA) and for the thawing season which corresponds to the period when air temperatures were above 0°C. The thawing index is the cumulative degree-days for air temperatures above 0°C. However, in 2012, the beginning of the thawing season was characterized by a period of oscillation above and below 0°C. The first daily air temperature above 0°C was recorded on May 3 and almost half the month of May has recorded values above 0°C. The daily air temperature was definitively above 0°C on May 31. In 2013, the daily air temperatures were above 0°C on two occasions: around May 20 (for 3 days) and at the beginning of June (for 2 days). The end of the thawing season is also characterized by a period of oscillation above and below 0°C, particularly for 2013 in which there were 10 consecutive days (Oct 13-22) where the daily air temperature was above 0°C.

Table 2: Climatic data recorded at the Environment Canada weather station AWOS (no. 2402591) for summer 2011, 2012, and 2013.

	2011	2012	2013
Thawing season (start and end dates)	June 2 - Sept 30	(May 3) May 31 – Oct 2	June 7 – Oct 4
Thawing season length (days)	121	125	120
Thawing index (°C-days)	704.2	729.3	619.1
Mean air temperature JJA / thawing season (°C)	6.7 / 5.9	6.7 / 6.1	5.9 / 5.2
Max air temperature JJA / thawing season (°C)	13.9 / 13.9	15.6 / 15.6	15.2 / 15.2
Min air temperature JJA / thawing season (°C)	-1.3 / -0.3	0.8 / 0.3	-4.4 / -1.7
Total precipitation JJA / thawing season (mm)	178 / 229	175 / 328.5	73.5 / 122

3.4 Permafrost sites

3.4.1 Ground and near-surface temperatures

In 2010, two boreholes were instrumented with thermistor cables from a depth of 0.25 m to depths of 3.3 and 15 m (IQAV4TC and IQAV2TC; Allard et al., 2014). At each site, a single-channel temperature logger, HOBO Pro v2 data logger manufactured by Onset® was used to measure the ground surface temperatures at 2-5 cm below the ground surface within a few centimetres from the thermistor cables (IQAV4HO and IQAV2HO; Allard et al., 2014). Ground temperatures from these two sites were used to visualise the progression of the thawing front and calculate the maximum active layer thickness (ALT) by linear interpolation of the temperature profile close to 0 °C (Riseborough, 2008). The accuracy is approximately 7 cm when active layer thickness is less than 100 cm (thermistor spacing of 25 cm), and about 14 cm when the active layer is more than 100 cm (thermistor spacing of 50 cm).

The borehole sites are located in two distinct areas. One is located within the Sylvia Grinnell (SG) Territorial Park adjacent to the airport (Figure 4). This area of the park is low lying, undisturbed, moist to wet, and vegetated with cotton grass and sedges. The thermistor cable is located less than 1 m from an ice wedge in a poorly drained marine deposit. Snow cover measured in March 2012 and 2013 was 20 and 40 cm respectively. The second borehole site is located near the Iqaluit airport (IA) runway, less than 6 m away from an ice wedge, in a well-drained glaciofluvial deposit (Figure 5). Snow cover is typically less than 2 cm. These two distinctive surface conditions will influence the onset and the end of the thawing and freezing seasons, and therefore, the thawing and freezing indices (Table 3).

Table 3: Ground surface thawing and freezing characteristics and maximum active layer thickness (ALT)[1] at two permafrost sites: Sylvia Grinnell (GT-SG) and Iqaluit airport (GT-IA).

	2010-2011		2011-2012		2012-2013	
	GT-SG	GT-IA	GT-SG	GT-IA	GT-SG	GT-IA
Thawing season (start and end dates)	June 3 – Oct 5	May 25 – Sept 30	May 27 – Oct 6	May 10 – Oct 3	June 12 – Oct 9	May 23 – Oct 5
Thawing season length (days)	125	129	133	147	120	136
Thawing index (°C-days)	627.8	937.2	681.2	1020.3	518.4	851.0
Freezing index (°C-days)	-2062.0	-2735.6	-2992.5	-3650.3	-1658.7	-3280.2
Max ALT (cm) (date)[2]	96 (Sept. 1)	139 (Sept. 1)	111 (Sept. 1)	139 (Aug. 26)	100 (Aug. 25)	129 (Aug. 25)

[1]Thawing, freezing and ALT derived from surface and ground temperatures.

[2]Date at which the maximum active layer thickness is reached.

3.4.2 Thaw tube and thaw settlement

Two thaw tubes were installed in summer 2010 (mid-August 2010) less than 3 m away from the thermistor cables GT-SG and GT-IA (Figures 4 and 5). Both thaw tubes are located towards the center of the ice wedge polygons. Thaw tube sites in this report are referenced as TT-SG and TT-IA.

Thaw tubes are used to measure heave and settlement of the ground surface. They consist of an outer PVC tube, anchored vertically in permafrost, and an inner clear plastic observation tube filled with deionized water (Nixon and Taylor, 1994). The inner tube is used to record the maximum active layer thickness (Table 4) while the heave and settlement are recorded by a scriber, attached to a sleeve, that scratches the outer PVC tube as it moves up and down with a metal grill resting on the ground surface. Except for year 2011, settlement measurements were recorded manually on the day, or very close to the day, of the satellite overpasses (Table 1). In summer 2011, measurements at thaw tubes sites were only made twice (end of July and end of September). Thaw tube markings are read with a precision of 1 mm. However, in reality, the grill resting on the ground may tilt and the mark on one side of the tube has been observed to differ from the opposite side by $\leq$ 5 mm. The accuracy of the thaw tube measurements is thus considered to be $\pm$ 5 mm.

In Table 4, the difference between ALT (relative to datum) and ALT (with settlement) in 2011 does not necessarily (especially for TT-SG) equal the total settlement occurred that summer since the heave (winter 2010-2011) observed at thaw tube sites is not considered. In subsequent years, the difference between ALT (relative to datum) and ALT (with settlement) is a combination of cumulative settlement since 2010 and heave (winters 2011-2012 and 2012-2013). Difference between thaw tube ALT (relative to datum) and ALT from GT sites is due to local soil and surface conditions, and the accuracy of the ALT based on ground temperatures.

Table 4: Maximum active layer thickness (ALT) at thaw tube sites: Sylvia Grinnell (TT-SG) and Iqaluit airport (TT-IA).

	2011		2012		2013	
	TT-SG	TT-IA	TT-SG	TT-IA	TT-SG	TT-IA
Max ALT (cm) (relative to the installation datum - 2010)	72	131	90	135	82	112
Max ALT (cm)[1] (with settlement)	64	130	77	133	70	111

[1]The date at which the maximum active layer thickness is reached is not known with this device.

3.4.3 Soil description

The permafrost site SG is located in a marine nearshore deposit (Mn ; Allard et al., 2012). The top soil is a layer of about 8 to 15 cm of organic matter (peat) underlain by fine sand with some gravels and pebbles (Figure 6a). A hand-portable drill was used to install the thermistor

cable and the thaw tube and to obtain intact permafrost cores below the thawing front and up to about 3.3 m. At the time the drillings were performed (Aug 8, 2010 for the GT-SG and Aug 16, 2010 for the TT-SG), the thawing front was at 60 cm at the GT-SG site and 45 cm at the TT-SG site. The soil stratigraphy is similar between the GT-SG and TT-SG sites, however, the ice content at the TT-SG site is higher. Visible ice (coating on particles) was observed within the active layer and below the thawing front while millimetric ice lenses are found around 85 cm (Figure 6b). Between 110 and 122 cm, the soil is particularly ice-rich (estimated to be around 60%) and corresponds to the permafrost table (Figure 6c). Up to 157 cm, the ice content decreases slightly, but the soil, fine grey sand with some gravels, still contains excess ice (Figure 6d). A thick layer of black organic matter is present just above 200 cm. This organic layer is covering a layer of fine to coarse brown sand with some gravels (Figure 6e) and a layer of fine to coarse grey sand up to the end of the boreholes (Figure 6f). Permafrost cores shown in Figure 6 are typical of sediments deposited in a littoral environment.

The permafrost site IA is located in a glaciomarine deposit (GMd ; Allard et al., 2012). The top soil is made of unsaturated, medium to coarse sand with some gravel. No permafrost cores are available for this site since the thermistor cable and the thaw tube were installed with an Air Track drill. Cuttings from the two boreholes indicate that the soil is made of brown, medium to coarse sand near the surface (Figure 7a) to medium to very fine grey sand at depth (15 m) (Figure 7b). Permafrost cores obtained nearby, in the same surficial geology unit, agree well with that description (Mathon-Dufour, 2014). In fact, at the IA site, the GMd probably corresponds to the foreset beds of the delta (Mathon-Dufour, 2014; Mathon-Dufour et al., 2015). Pore ice is the main type of ice within the active layer at this site.

4 METHOD

DInSAR is based on the principle that local surface elevation can be detected and measured from returning active microwave radar signals transmitted from a satellite to a reflective surface on the Earth. From the analysis of the phase difference between repeat-track synthetic aperture radar (SAR) acquisitions separated by a time interval (visualised as interferograms), the surface displacement in the SAR line-of-sight (LOS) can be calculated. DInSAR results were generated using both a simple time series of interferograms spanning consecutive time intervals of 24 and sometimes 48 days, and a stacking approach which averages multiple temporally overlapping interferograms to reduce noise and bring out subtle trends. The time series at selected sites (pixels) were used for point comparison with thaw tube measurements while the stacking approach is used to produce large area maps of seasonal ground displacement. In the stacking approach all good quality interferograms possible within the summer data set were used (Table 5). In relatively flat areas like most of the terrain in Iqaluit, satellite geometry can be used to convert the LOS observation to a vertical displacement. Further details on data processing can be found in Short et al. (2011, 2014).

Table 5: RADARSAT-2 data pairs (interferograms) for years 2011, 2012, and 2013.

2011 DInSAR pair (yyyymmdd-yyyymmdd)	2012 DInSAR pair (yyyymmdd-yyyymmdd)	2013 DInSAR pair (yyyymmdd-yyyymmdd)
20110622-20110716	20120523-20120616	20130611-20130705
20110716-20110809	20120616-20120710	20130705-20130729
20110716-20110902	20120710-20120803	20130705-20130822
20110716-20110926	20120803-20120827	20130729-20130822
20110809-20110902	20120827-20120920	20130729-20130915
20110809-20110926	20120710-20120827	20130822-20130915
20110902-20110926	20120803-20120920	
	20120710-20120920	

In a Geographical Information System (GIS), DInSAR displacements were statistically analysed using the surficial geology polygons (updated version of Allard et al., 2012) and the built and natural areas. The built areas include the delineation of the municipal and airport infrastructure provided by the City of Iqaluit in 2010. Roads, individual buildings and houses were combined into one polygon since the terrain between infrastructure is potentially disturbed. In addition, a buffer of 5 m was applied around infrastructure. Figure 8 shows the footprints of the built (urban) and the natural areas with surficial geology as the background.

5 RESULTS

5.1 DInSAR seasonal surface displacement maps for 2011, 2012 and 2013

Seasonal surface displacement maps derived from stacked RADARSAT-2 DInSAR for summers 2011, 2012, and 2013 are shown in Figure 9, 10, and 11 respectively. The units are vertical centimetres, with negative values indicating downward movement of the ground. The displacements are relative to a reference point assumed to be stable, in this case the bedrock area marked with a star. In this way regional effects such as glacio-isostatic adjustment are not detected, because the reference point would be equally affected (Short et al. 2014). Each displacement measurement in the resultant DInSAR map represents an area (pixel) of approximately 1.8 by 1.6 m on the ground, and is a smoothed product of neighbouring pixels. The margin of error for the maps has been established as ± 1 cm and displacement within this range is considered insignificant and mapped as stable (Short et al., 2014). The same vertical displacement classes chosen in Short et al. (2014) were used in this study to facilitate the comparison. The class “no data” represents a loss of coherence, meaning that the surface characteristics significantly changed (e.g. construction or destruction) between repeat SAR acquisitions, or the surface is water or other smooth materials producing specular scattering and resulting in coherence loss.

Similarities are observed between years in the patterns of displacement which correlate well with the surficial geology. In general, the displacements were higher in 2012, especially in the town and southwest of the airport. The difference between the three years is partly related to the

difference in the time period of satellite acquisitions which is one month longer in 2012 (Table 1). However, the difference can also be explained by the length of the thaw season in 2012, its early start compared to 2011 and 2013, the higher air and ground surface thawing indices (Tables 2 and 3), and thicker active layer (Table 3). Other factors such as water level changes at the surface (see section 6 – Discussion) may also explain the difference.

The 2012 and 2013 data are noisier than the 2011 dataset, possibly influenced by the inclusion of late spring scenes with residual snow melt. Only the processing of 2012 data yielded results directly over the Iqaluit airport infrastructure, in 2011 and 2013 the paved surfaces were characterised by coherence loss.

5.2 DInSAR time series for 2011, 2012 and 2013 at permafrost sites

The DInSAR time series are shown in Figures 12 to 14 for both permafrost sites TT-SG and TT-IA each year. These plots can be noisy since there is no stacking and hence no reduction of atmospheric noise, and there is less local area averaging than in the map products; further discussion on the error estimation of the DInSAR time series data can be found in Short et al. (2014). Also shown in Figures 12 to 14 are air and ground surface temperatures, precipitation, cumulative degree-days of thawing/freezing (thawing and freezing indices), active layer thickness, and cumulative displacement from the thaw tubes TT-SG and TT-IA.

In summer 2011, the calculated DInSAR displacements were lower than the settlement values observed at TT-SG and TT-IA. One of the main reasons for this discrepancy is the late start of SAR acquisition, about one month (June 22; Table 1) after the onset of ground surface thawing (end of May/beginning of June; Table 3). Active layer thickness increases rapidly at the beginning of the thawing season. Assuming TT-IA (and GT-IA) have (1) only pore ice (and no massive ice), (2) an unsaturated near-surface, and (3) a thawing front advance of about 55 cm between the onset of ground surface thawing and the first SAR acquisition, the settlement could be estimated at <0.6 cm, which is lower (but within the thaw tube accuracy) than the difference between the observed displacement and that calculated by DInSAR on June 22 (~1 cm). At GT-SG, even if the thawing front advance was only 35 cm prior to the first SAR acquisition (probably slightly less at TT-SG due to higher ice content), there is likely excess ice within the active layer which is composed of saturated peat and fine sand with millimetric ice lenses. This could lead to more settlement at TT-SG than at TT-IA and to a greater discrepancy between the observed displacement and the one calculated by DInSAR on June 22.

In 2012 and 2013, the first SAR acquisition was closer in time to the start of the thawing season. This is particularly true at TT-SG while at TT-IA the ground surface started to thaw 13 and 19 days before the SAR acquisition for 2012 and 2013 respectively (Tables 1 and 3). In 2012, there was an early warm wave at GT-IA (and TT-IA) which initiated the thaw of about 30 cm of soil closely followed by a settlement of 1 cm. Even if the ground was fully saturated with pore ice (which is probably not the case), this amount of settlement (1 cm for 30 cm of thaw soil) seems too high given the soil conditions, but it remains plausible taking into account the accuracy of the thaw tube measurements. In 2013, the thawing front at GT-IA was at 48 cm

(probably slightly less at TT-IA if we compared with ALT in Table 4; 112 vs. 129 cm) when the SAR acquisitions started. This time, there was not much settlement associated with the thawing of the ground, probably due to the dryness of the soil. In both years, when the start date of settlement at TT-IA is reset to coincide with the SAR acquisition, the calculated (DInSAR) displacement is slightly greater than the observed (thaw tube) settlement, but remains close to the thaw tube accuracy, and the observed settlement is within the DInSAR margin of error. At GT-SG (and TT-SG), although the ground thawing and the settlement started 4 and 1 days after the SAR acquisition, the discrepancy between the two sets of measurements remains higher than the thaw tube accuracy or the DInSAR margin of error. Possible explanations for this discrepancy are given in Short et al. (2014) and could be attributed to lower accuracies in areas prone to saturation and flooding, due to pockets of low coherence and the effects of data filtering and interpolation.

If we compare the years with each other (Figures 12 to 14), the observed settlement at the end of the thawing season at TT-IA is slightly lower in 2011 (-1.9 cm) than 2012 (-2.35 cm) and even lower in 2013 (-1.1 cm), while the DInSAR derived settlements at TT-IA increase each year; from -0.48 cm (2011) to -1.88 (2013). The active layer thickness calculated from ground temperatures is the same in 2011 and 2012 (GT-IA, Table 3) or about the same at TT-IA (Table 4) and slightly thinner in 2013. Therefore, the trend in observed settlements through the years is reasonable while the one from calculated DInSAR displacements is not yet understood.

At the SG site, from thaw tube results, there is less settlement in 2012 (-8.5 cm) than in 2011 (-11.8 cm), even if the active layer thickness is greater in 2012 (at GT-SG and TT-SG; Table 4). One possible explanation could be related to the preceding freezing season and the hydrological conditions within the active layer. Fall and winter 2010-2011 were characterised by a lower ground surface freezing index and a lower rate of cooling at the beginning of the freezing season than 2011-2012 (Table 3; Figures 12 and 13). Knowing that the ground is wet and saturated at the onset of freezing, this slow cooling rate could have fostered the development of ice lenses within the active layer (Harris, 1981), leading to more settlement the following summer (2011). In fall-winter 2011-2012, the cooling rate was much higher and occurred earlier at the beginning of the freezing season, therefore, the development of ice lenses could have been partly inhibited. In 2012-2013, the ground surface freezing index was the lowest of the 3 years and the cooling rate was between the ones in fall 2010 and 2012; however, the lower settlement observed at the thaw tube (-5.6 cm) is probably better correlated to the very low ground surface thawing index in 2013. Long term data analysis in conjunction with climatic data and soil characteristics will be needed to confirm the link between the preceding freezing season and settlement. At the same site, the calculated DInSAR time series results do not seem to follow a logical trend through the years based on air temperature data. Although the displacement was higher in 2012 (-2.6 cm) than 2011 (-2.1 cm), the one in 2013 (-2.3 cm) was slightly higher than 2011. Beside the distortion due to the variable time span of the DInSAR acquisitions, changes in the precipitation regime between the years could also influence the DInSAR results in this poorly drained area.

In 2013, for both sites, the cumulative displacement curves from the thaw tube measurements respond accordingly to the onset of the ground freezing season and the freeze back of the active layer (Figure 12; see the vertical black dashed line). At TT-SG, the cumulative displacement (uplift) from DInSAR, calculated between August 22nd and September 15th, could be influenced by another parameter such as change in surface water levels.

5.3 Correlation with surficial geology

Histograms of the percentage of each class of displacement per surficial geology unit and for each year are given in Figure 15. Results are consistent from one year to the next and are also in agreement with the subset analysis done with the 2012 DInSAR for the Iqaluit airport area (Short at al., 2014). Bedrock (R) and Till veneer on Bedrock (Tv/R) are seen to be very stable (81 to 91% and 70 to 82%, respectively). The Till blanket (Tb) unit is composed of coarse sediment within a fine-grained matrix which was found to be ice-rich. Ground located in this unit is less stable (37 to 47%) and higher displacements are observed than the Tv/R unit. Glaciofluvial (GFp and GFr) sediments are comprised of sands and gravels and are well drained and therefore generally not thaw sensitive. This is reflected by the high proportion of stable ground (56 to 69% for GFp and 70 to 76% for GFr) within this unit. However, these units can also contain ice wedges and massive ice bodies (at least one massive ice body has been observed in GFp at high elevation) which would introduce localised instability. Alluvial (Ap and At) and Glaciomarine (GMd) sediments are mixed soils, with grain size ranging from boulder to silt particle. Although half of the pixels from these three units are within the stable class (38 to 55%), a larger proportion of the displacement pixels within these units are in the -1 to -2.5 cm class which represent normal settlement values for ice-poor sediments (containing pore ice only). Displacement values greater than -2.5 cm for Ap, At and GMd terrain units can be explained by localised settlement. For example GMd is affected by extensive ice wedge polygons. Short et al. (2014) have shown that DInSAR displacements appear to capture settlement in the vicinity of some frost cracks associated with pre-construction ice wedges. In addition, the silty GMd sediments were found to be ice-rich (segregation ice) in several locations (Mathon-Dufour et al., 2015). For Ap and At, displacements greater than -2.5 cm could be attributed to the underlying unit such as GMd sediments. Lacustrine (Lv) sediments, fine grained and prone to water retention, are frost susceptible and likely ice-rich at the permafrost table (Mathon-Dufour et al., 2015). Nearshore marine (Mn) is composed of sand and gravel deposited as beaches and should be ice-poor. However, the top layer is made of fine and ice-rich sediments (see Figure 6c). Oldenborger et al. (2015) also show that the top layer of Mn sediments can be locally highly resistive and interpreted as ice-rich. Lv and Mn form the least stable terrain with 7 to 28% (Lv) and 14 to 27% (Mn) of these areas showing more than -2.5 cm of seasonal displacement. Marine veneer (Mv) sediments which are composed of sand and gravel characterised by beach ridges tend to be stable (41 to 67%). This unit, mainly mapped in the Apex sector, probably covers the GMd unit where ice wedges may occasionally be present. Littoral and nearshore marine (Mr) sediments formed the actual beaches where permafrost may be present. This unit is mostly stable

(57 to 69%) and small displacements could be attributed to sediment movements and beach dryness/wetness. Small patches of organic material (O) have been mapped in the area of Iqaluit. This unit is found in poorly drained sites and should be ice-rich, and therefore associated with a higher percentage of displacement values greater than -2.5 cm (9 to 15%) for this type of terrain.

5.4 Comparison between urban and natural terrain

Results above are obtained without differentiation between built, or urban, and natural terrain. If displacements are separated into these two environments, the histograms are still dominated by low displacements (less than -2.5 cm) (Figure 16) as seen previously when results were analysed in conjunction with surficial geology (Figure 15). In general, among the three years, the stable class is slightly higher (7 to 20%) for natural than for urban areas due to the higher percentage of R and Tv/R units in natural terrain (Figure 17). Residential areas including all built areas in Iqaluit (except the Iqaluit airport) are mainly built on the Mn unit while the Iqaluit airport is built on GMd (Figures 17 and 3). Isolating these two units respectively for urban and natural terrain shows that the percentage of stable pixels is generally higher in built areas than in the natural environment and inversely displacements greater than -2.5 cm are more frequent in natural terrain (Figure 18). This is particularly true for sediment types showing greater amount of higher displacements, as units that are generally stable, often ice-poor, remain stable even if their surfaces are modified. Lv, among the least stable unit, follows the same pattern of displacement between urban and natural terrain as Mn and GMd (Figure 19). The total surface areas occupied by Mn and GMd in natural terrain are slightly higher than in built areas whereas for Lv it is the opposite (Figures 18 and 19).

6 DISCUSSION

Between years there is a clear similarity in the patterns of displacement in relation to surficial geology. Therefore, DInSAR results should always be interpreted first by looking at the surficial geology. Schaefer et al. (2015) used DInSAR results to derive ALT regardless of the surficial geology, but conclude that gravel and well-drained sediments contributed to the underestimation of the ALT in their model. Our observations show that local ground ice features (e.g. ice wedges) or ice-rich soil can contribute to the variability in displacement values within the same unit (Short et al., 2014; LeBlanc et al., 2015). Other parameters such as groundwater flow within the active layer (Short et al., 2014) can also influence the variability in displacement values for a given surficial geology. Furthermore, LeBlanc et al. (2015) show that a more detailed surficial geology map, covering a portion of the eastern town of Iqaluit towards the northeast of the town, could explain displacement patterns observed at a finer scale. It is shown that displacements greater than -2.5 cm are mainly associated with alluvial sediments (A), glaciofluvial boulder fields (GF boulder field), and organic deposits (O) (Figure 2 in LeBlanc et al., 2015) rather than being associated with Tb, Tv, and GFp (Figure 3). Higher resolution mapping of organic material would likely increase, for that unit, the percentage of displacement values greater than -2.5 cm, otherwise attributed to other surficial units from Figure 3. The displacements in the cases of A

and GF boulder field could be correlated with water level changes at the surface since these two units are likely not frost susceptible. Surface water was typically observed in these units (Figure 20). This could explain why the 2013 DInSAR data are showing greater amount of high displacements northeast of Iqaluit despite a colder and shorter thawing season. Total precipitation in 2013 (Figure 14, Table 2) was lower than in 2011 and 2012 (Figure 12 and 13, Table 2). Rainy summers will lead to a greater amount of water at the surface of the ground which could mask the true (and greater) settlement.

Some discrepancy between years can be explained by climatic data when displacements were examined at the two permafrost sites. In addition to the possible influence that the preceding freezing season could play, change in surface water due to the thawing of active layer over the course of summers combined with the occurrence of precipitation might also influence the calculated displacements. The detection by DInSAR of seasonal variation in water level in other permafrost environment has been noticed by Short et al. (2012b) and Schaefer et al. (2015), but was not considered as the plausible explanation for the discrepancy at the SG site in year 2012 (Short et al., 2014). However, the uplift displacement seen in the DInSAR time series compared to the downward displacement at TT-SG in 2013 and the high displacement calculated by DInSAR in relatively stable terrain such as the glaciofluvial boulder field shows that seasonal variation in water level should be investigated in order to more fully understand the causes of displacements calculated by DInSAR.

Unfortunately, the DInSAR time series are noisier than the stacking approach (map), and this adds to the complexity of the interpretation. While the agreement with the DInSAR time series and the thaw tube measurements is disappointing, the time series do consistently identify that the settlement at the TT-SG site is greater than the TT-IA, thus qualitatively in agreement. The poor agreement of the time series results is reduced in the stacked map products, where the averaging of many input data sets and local area smoothing produces total settlement rates that are closer to the thaw tube measurements (e.g. Short et al., 2012a; Short et al., 2014).

The histogram similarity between built and natural terrains is related to the surficial geology units on which each environment is located; for example, for Iqaluit, the main surficial unit is different for urban and natural terrain. However, the results show that for a given surficial geology unit, displacements were generally lower in built areas than in the natural environment. Granular fill or pads and construction methods play a role in reducing the amount of settlement if the base of the active layer is maintained above the natural ground. On the other hand, the active layer under a paved road can be thicker (e.g. Mathon-Dufour et al., 2015) leading to more settlement, especially for thaw-sensitive soil such as Lv. However, DInSAR displacements were not higher under paved infrastructure. Except for the year 2012, most of the largest paved areas (e.g. the Iqaluit airport) were classified as “no data”. These “no data” probably contribute to an underestimation of the percentage of higher displacements since severe settlements affecting the airport infrastructure have been observed. Even in 2012 where “no data” over the Iqaluit airport was minimal, some paved areas experiencing settlement were observed to be frequently filled with water. These water pockets would cause coherence loss (“no data”) and phase filtering

would likely smooth and underestimate the true displacement signal (Short et al., 2014). This is particularly true at locations covered by GMd on aprons, but not necessarily for Lv mapped mainly under the runway and one of the main taxiways for which the surface is generally kept dry. In many areas, at the airport facility, ice-rich sediments were found just below the base of the active layer or at the top of the permafrost table (Mathon-Dufour et al., 2015). Consequently, even if the granular embankment appears to limit the amount of high displacement compared to the natural terrain, it could only be a matter of time before the situation is reversed.

Conventional DInSAR processing might not reproduce with exactitude the true displacement especially in areas prone to saturation and flooding (Short et al., 2014), but the results can certainly be used for identification of thaw-sensitive areas or at least difficult terrain for construction (e.g. in the case of surface water). To locate thaw-sensitive soils and/or difficult terrain, one DInSAR season can be used because of the similarity between years in the patterns of displacement. However, more than one season helps to differentiate between different causes of displacement (due to thaw-sensitive ground, change in surface water or both). In light of our current findings, using DInSAR to assess other parameters, such as ALT, with high confidence, might depend on the complexity of the terrain and what additional ground-based observations are available.

7 CONCLUSIONS

The main results from this study are:

1- Interannual results from the Iqaluit area show that one DInSAR season could be used to locate thaw-sensitive soils and/or difficult terrain for construction because of the similarity between years in the patterns of displacement.

2- Surficial geology and ground ice are essential information to interpret DInSAR results. The mapping scale of surficial deposits can explain why some displacement patterns are not well explained, but would be at a different scale. Other parameters such as seasonal change in water level at the surface could also influence the DInSAR results.

3- The analysis of more than one season in conjunction with climatic data can confirm the patterns of displacement and help to differentiate between different causes of displacement (e.g. ground ice melt vs. change in water level at the surface and the impact of the preceding freezing season conditions).

4- For a given surficial geology unit, displacements were generally lower in built areas than in the natural environment, likely due to construction materials and methods. This can be characteristic to cold and continuous permafrost environments and the situation may be reversed in time.

Since InSAR is an emerging technology, its application to permafrost terrain will certainly improve the way permafrost is characterized at a useful scale for infrastructure monitoring and for assessing terrain for resource development. Findings from this study can be used to guide these DInSAR applications.

8 ACKNOWLEDGEMENTS

Funding was provided by Natural Resources Canada Climate Change Geoscience Program and the Canada-Nunavut Geoscience Office through the Canadian Northern Economic Development Agency's (CanNor) Strategic Investments in Northern Economic Development (SINED). Special thanks go to M. Allard and E. L'Hérault for their contribution of ground data as well as to T. Irniq, J. Davidee (Arctic College), J. Shirley (Nunavut Research Institute), T. Tremblay, R. Hinanik, and K. Napayok (Canada-Nunavut Geoscience Office) for their help in the field with thaw tube measurements. The authors would also like to express their thanks to J. Hawkins and K. Henderson, from the Iqaluit International Airport, and their staff. RADARSAT-2 data are copyright MacDonald, Dettwiler and Associates and were provided by the Canadian Space Agency.

9 REFERENCES

Allard, M., Doyon, J., Mathon-Dufour, V., LeBlanc, A.-M., L'Hérault, E., Mate, D., Oldenborger, G.A., and Sladen, W.E. 2012. Surficial geology, Iqaluit, Nunavut; *Geological Survey of Canada, Canadian Geoscience Map 64 (preliminary version)*, scale 1:15 000.

Allard, M., Sarrazin, D., L'Hérault, E. 2014. Borehole monitoring temperatures in northeastern Canada, v. 1.2 (1988-2014). Nordicana D8, doi: 10.5885/45291SL-34F28A9491014AFD.

Harris, C. 1981. Periglacial mass-wasting : a review of research. British Geomorphological Research Group, Research Monograph 4. Geo Abstract, Norwich, 204 pp.

Heginbottom, J.A., Dubreuil, M.A. and Harker, P.A. 1995. Canada – Permafrost, In: National Atlas of Canada, 5th Edition, National Atlas Information Service, Natural Resources Canada, MCR 4177.

LeBlanc, A.-M., Short, N., Mathon-Dufour, V., Allard, M., Tremblay, T., Oldenborger, G.A., and Chartrand, J. 2015. DInSAR seasonal surface displacement in built and natural permafrost environments, Iqaluit, Nunavut, Canada. *Proceedings of GeoQuébec 2015, Québec city, Canada, Sept. 20-23, 2015.*

Mathon-Dufour, V., Allard, M., and LeBlanc, A.-M. 2015. Assessment of permafrost conditions in support of the rehabilitation and adaptation to climate change of the Iqaluit airport, Nunavut, Canada. *Proceedings of GeoQuébec 2015, Québec city, Canada, Sept. 20-23, 2015.*

Oldenborger, G.A., LeBlanc, A-M., and Sladen, W.E. 2015. Electrical and electromagnetic data for permafrost characterization at Iqaluit International Airport, Nunavut; *Geological Survey of Canada, Open File 7750*: 41 p.

Schaefer, K., Liu, L., Parsekian, A., Jafarov, E., Chen, A., Zhang, T., Gusmeroli, A., Panda, S., Zebker, H.A. and Schaefer, T. 2015. Remotely Sensed Active Layer Thickness

(ReSALT) at Barrow, Alaska Using Interferometric Synthetic Aperture Radar. *Remote Sensing*, 7: 3735-3759.

Short, N., Brisco, B., Couture, N., Pollard, W., Murnaghan, K. and Budkewitsch, P. 2011. A comparison of TerraSAR-X, RADARSAT-2 and ALOS-PALSAR interferometry for monitoring permafrost environments, case study from Herschel Island, Canada. Remote Sensing of Environment, 115, 3491–3506, doi:10.1016/j.rse.2011.08.012.

Short, N., LeBlanc, A.-M., Sladen, W.E., Allard, M. and Mathon-Dufour, V. 2012a. Seasonal Surface Displacement Derived from InSAR, Iqaluit, Nunavut; *Geological Survey of Canada, Canadian Geoscience Map 66*.

Short, N., B. Brisco and K. Murnaghan, 2012b. Monitoring Permafrost Environments with InSAR and Polarimetry, Case Studies from Canada, Proceedings of the IEEE International Geoscience and Remote Sensing Symposium, July 22-27, 2012, Munich, Germany.

Short, N., LeBlanc, A.-M. Sladen, W.E., Mathon-Dufour, V., Oldenborger, G.A. and Brisco, B. 2014. RADARSAT-2 D-InSAR for ground displacement in permafrost terrain, validation from Iqaluit Airport, Baffin Island, Canada. *Remote Sensing of Environment,* 141, 40-51.

Short, S.K. and Jacobs, J.D. 1982. A 1100 year paleoclimatic record from Burton Bay-Tarr Inlet, Baffin Island. *Canadian Journal of Earth Science,* 19, 398-409.

St-Onge, M.R., Jackson, G.D. and Henderson, I. 2006. Geology, Baffin Island (south of 70°N and east of 80°W), Nunavut; *Geological Survey of Canada, Open File 4931*, scale 1:500 000.

FIGURES

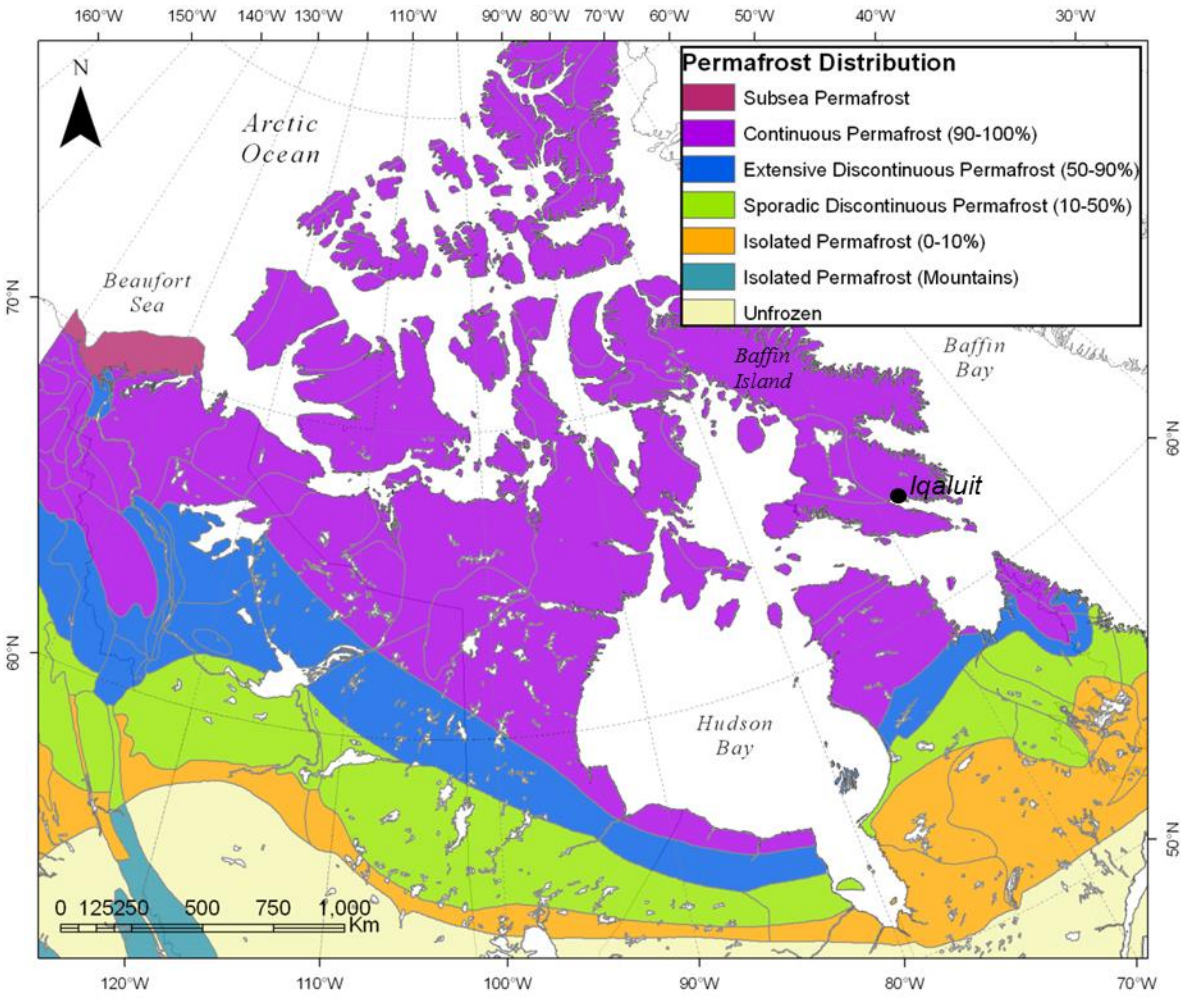

Figure 1: Permafrost map of Canada (modified from Heginbottom et al. 1995). Iqaluit is located on southeastern Baffin Island.

Figure 2: Examples of buildings built on a) steel piles and embankment pad, b) concrete slab on embankment pad, and c) concrete piles and embankment pad.

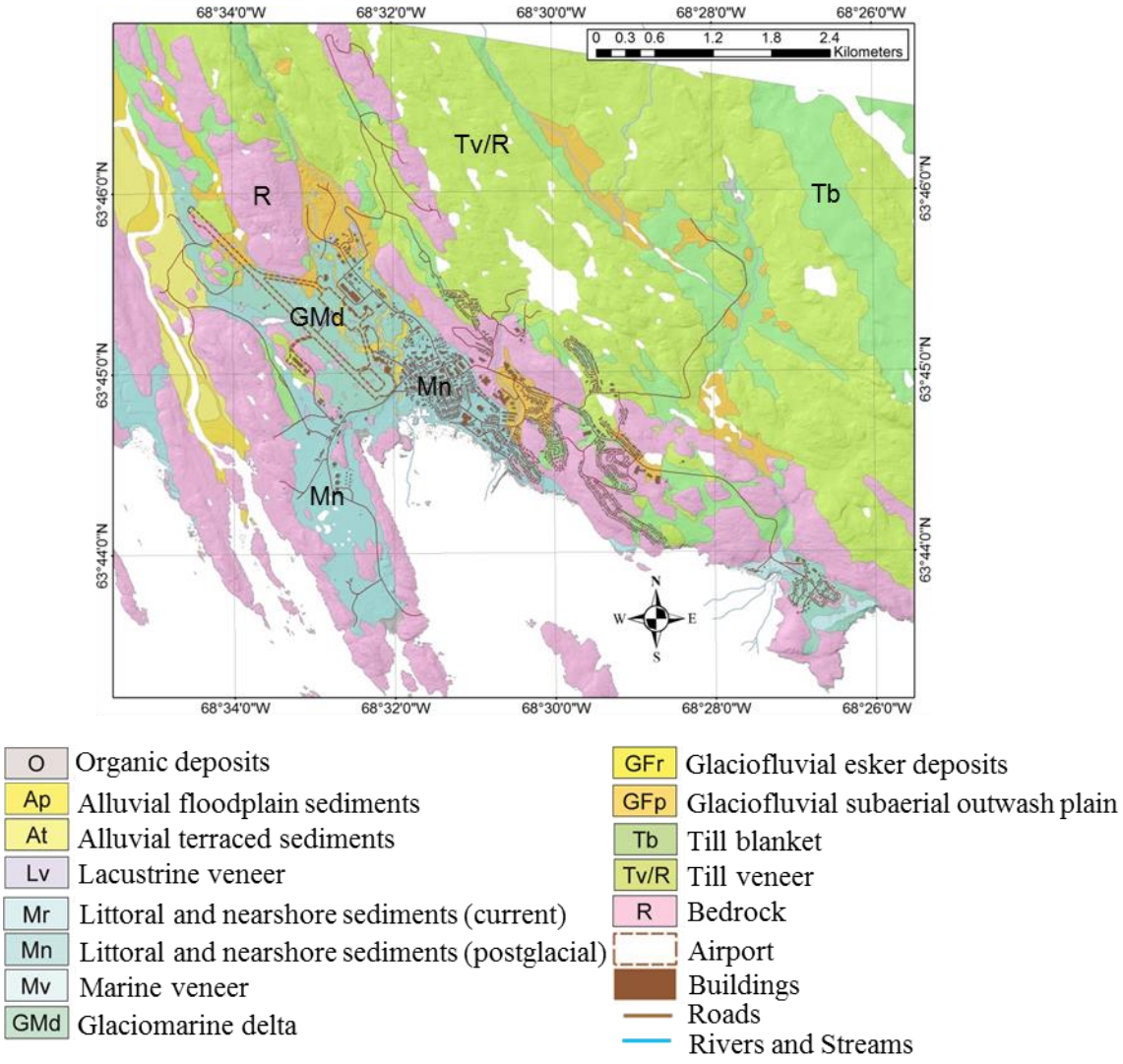

Figure 3: Surficial Geology of Iqaluit (modified from Allard et al. 2012 and Mathon-Dufour et al. 2015). Background shaded relief from 1m DEM created with proprietary stereo image (WorldView-1) matching process by PhotoSat Ltd.

Figure 4: Sylvia Grinnell (SG) site. In background, the thermistor cable, in foreground, the thaw tube.

Figure 5: Iqaluit Airport (IA) site. In background, the thermistor cable, in foreground, the thaw tube.

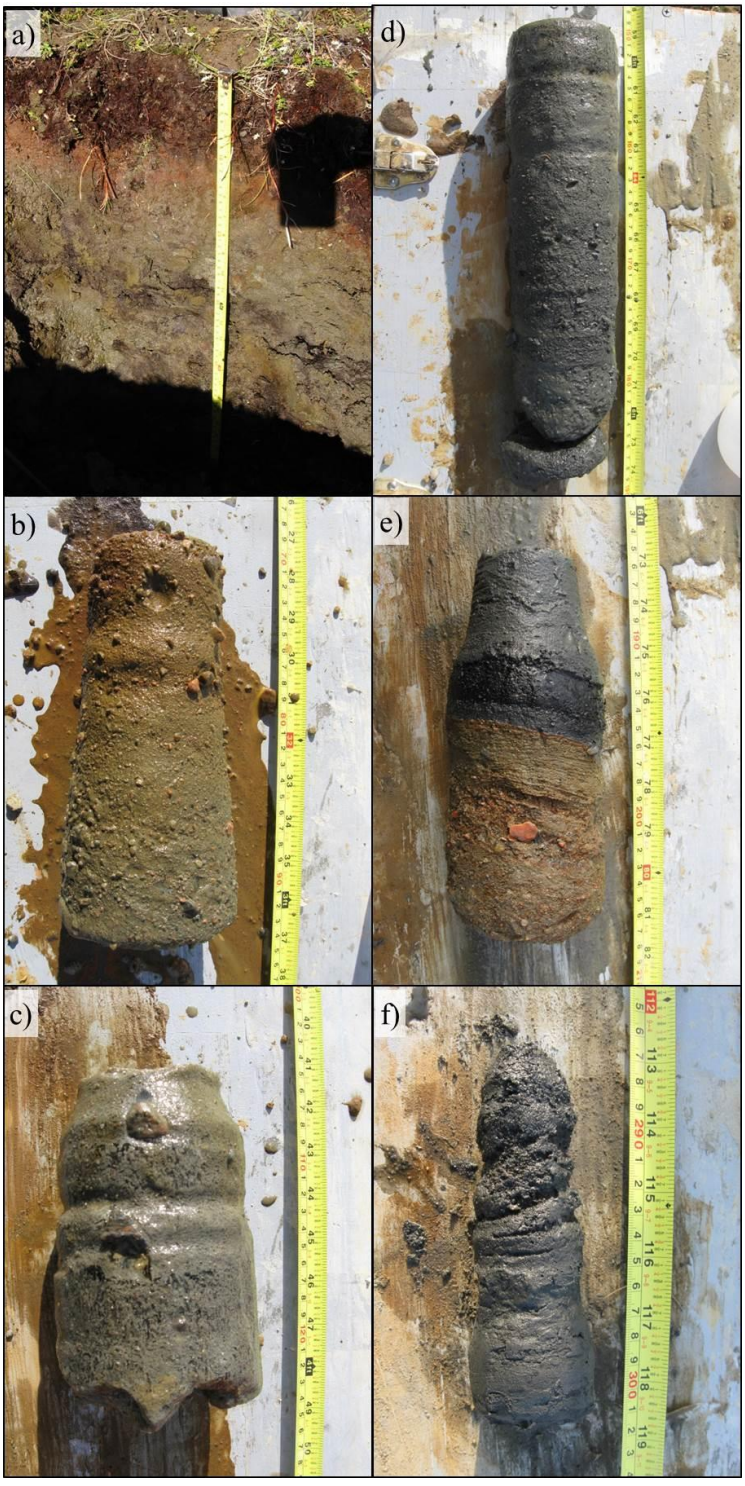

Figure 6: Sylvia Grinnell (SG) permafrost site: a) top soil, b) active layer core, c) ice-rich permafrost core (permafrost table), d) permafrost core between 152 and 186 cm, e) permafrost core between 186 and 205 cm, f) permafrost core between 286 and 300 cm.

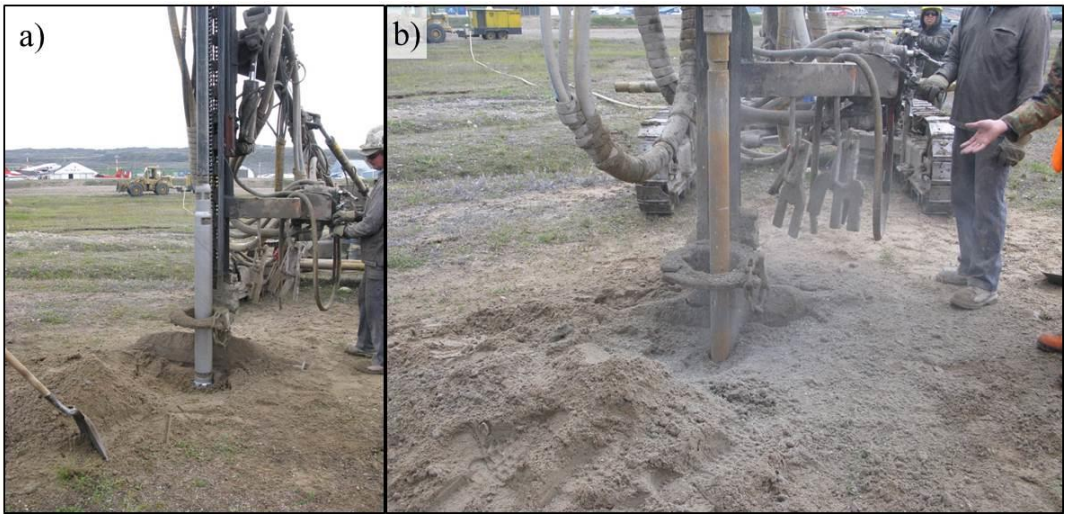

Figure 7: Iqaluit Airport (IA) permafrost site: a) brown sand cuttings and b) grey sand cuttings.

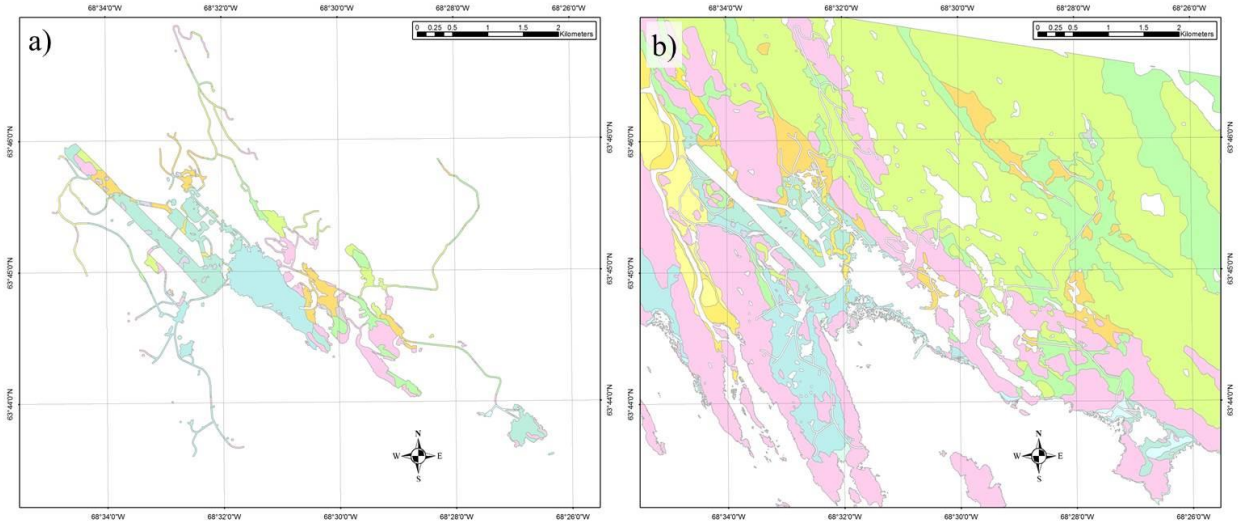

Figure 8: Footprints of the built (a) and the natural (b) areas with the surficial geology of Iqaluit as the background.

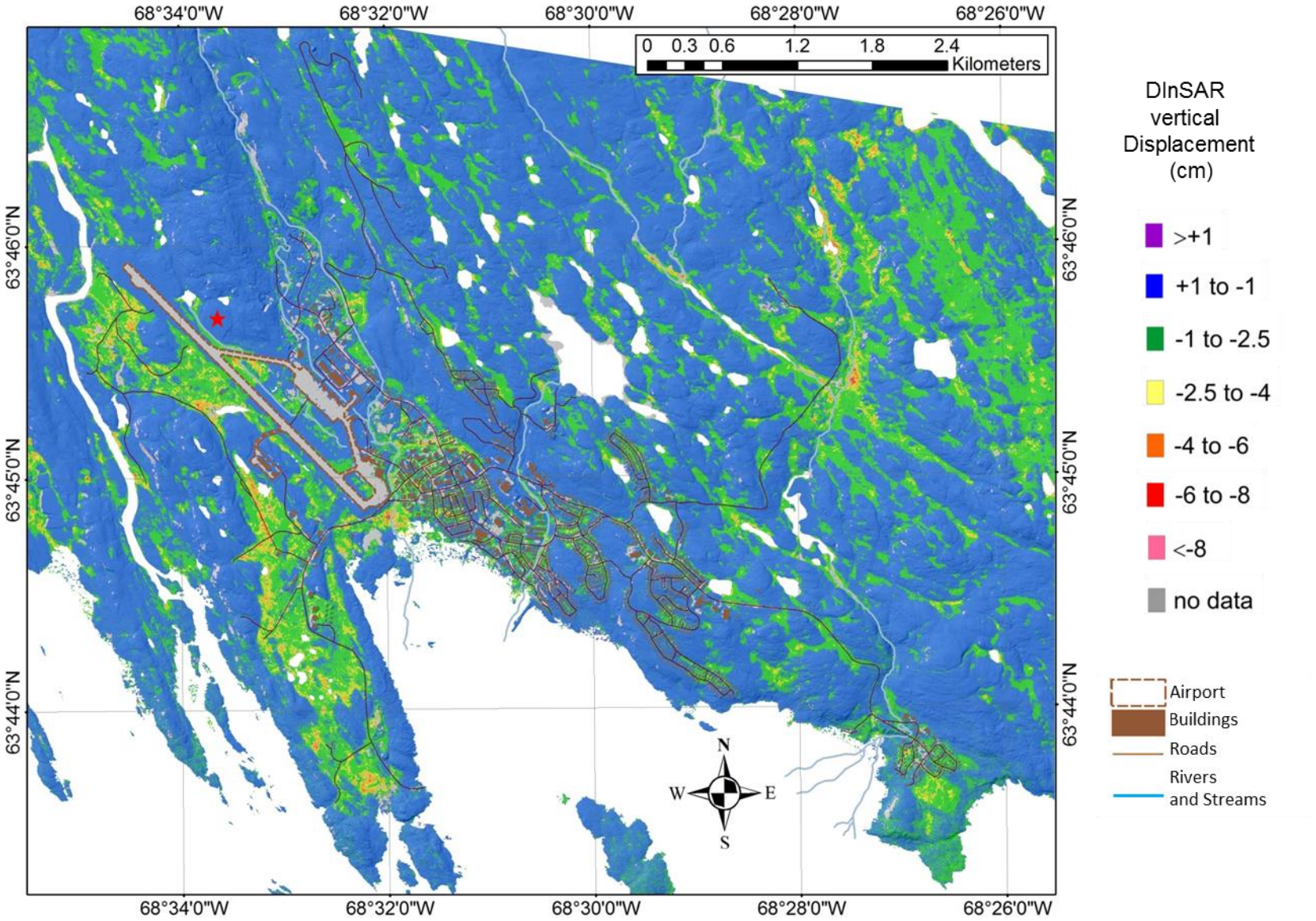

Figure 9: DInSAR seasonal surface displacement for Iqaluit for year 2011.

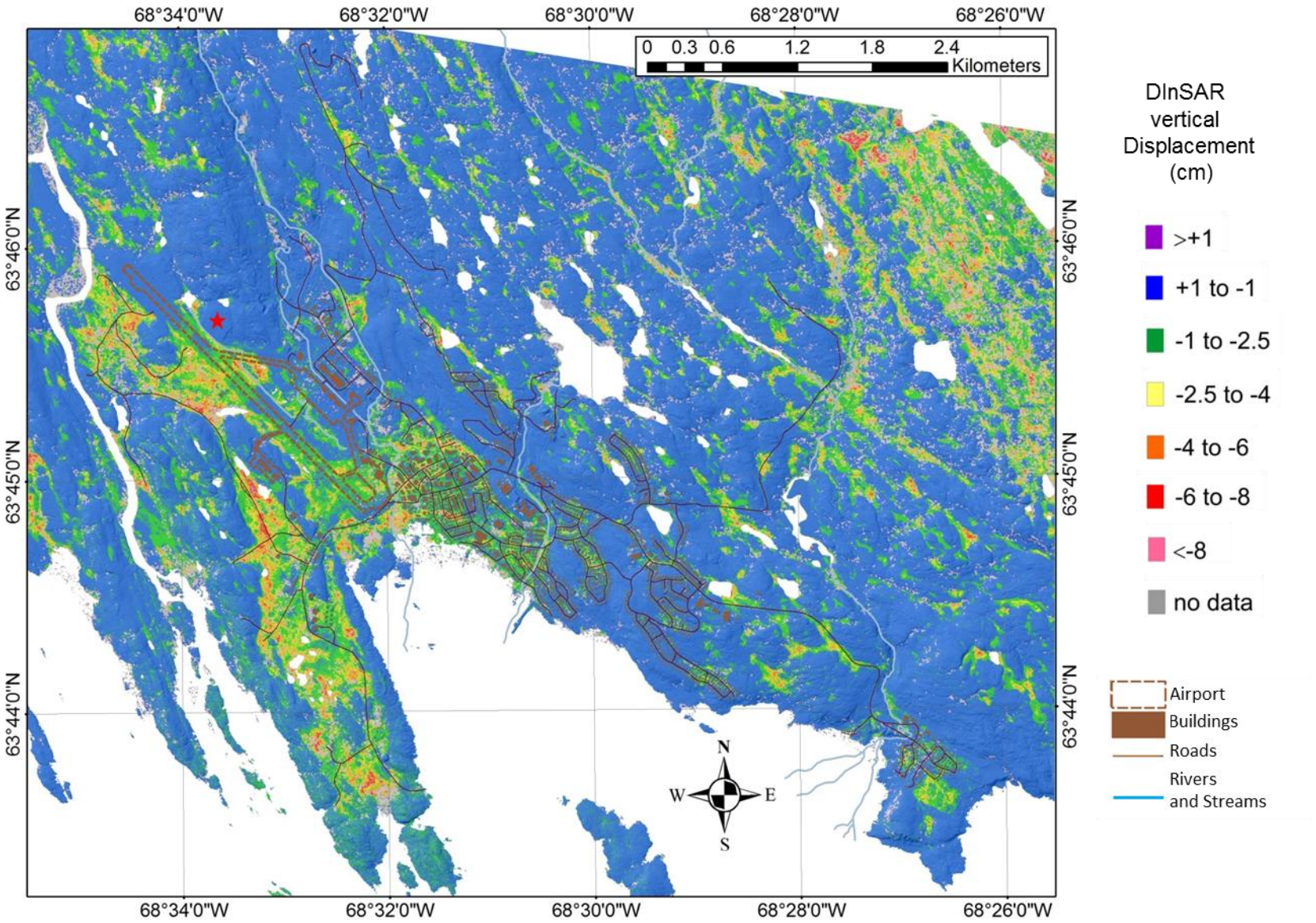

Figure 10: DInSAR seasonal surface displacement for Iqaluit for year 2012.

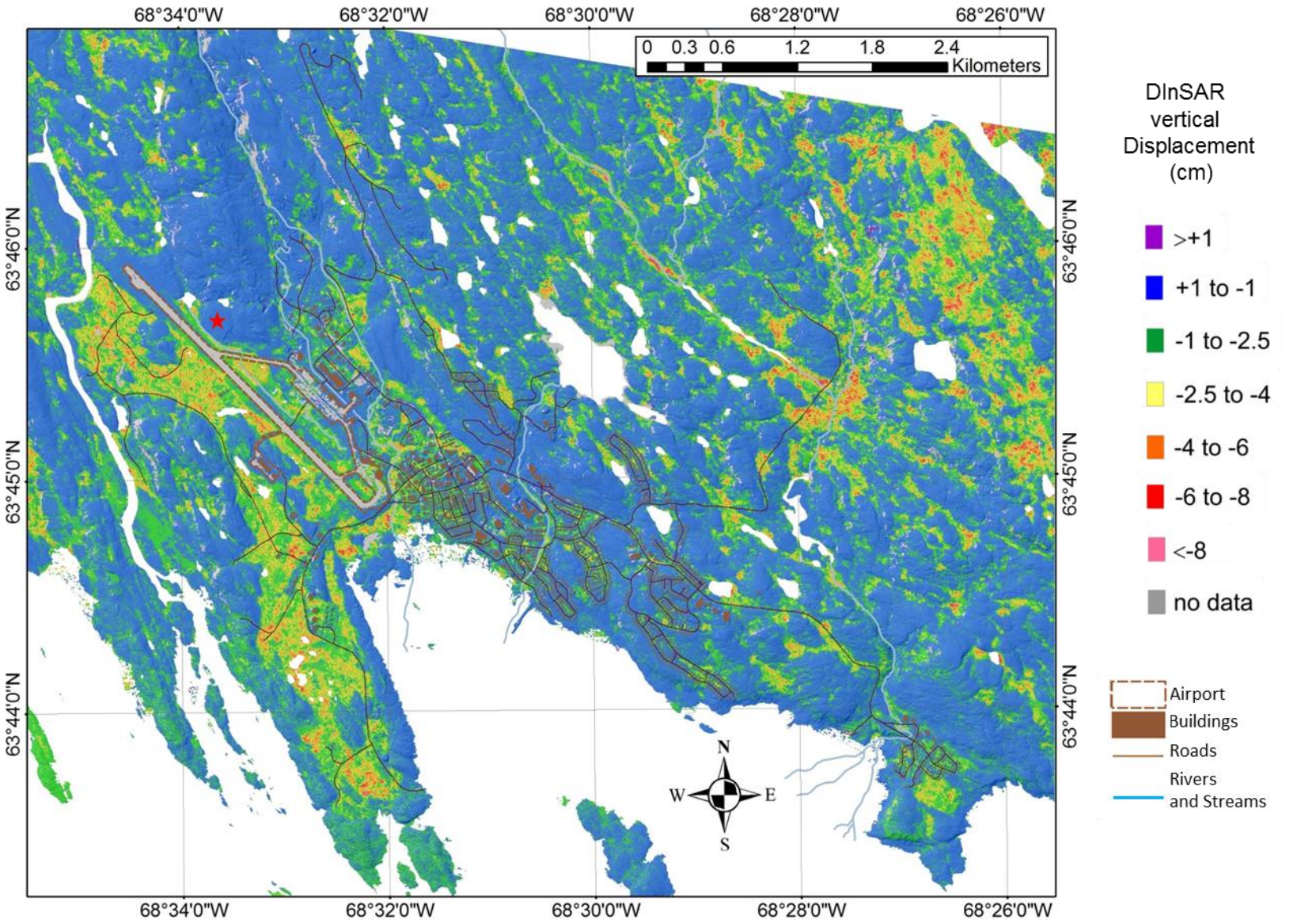

Figure 11: DInSAR seasonal surface displacement for Iqaluit for year 2013.

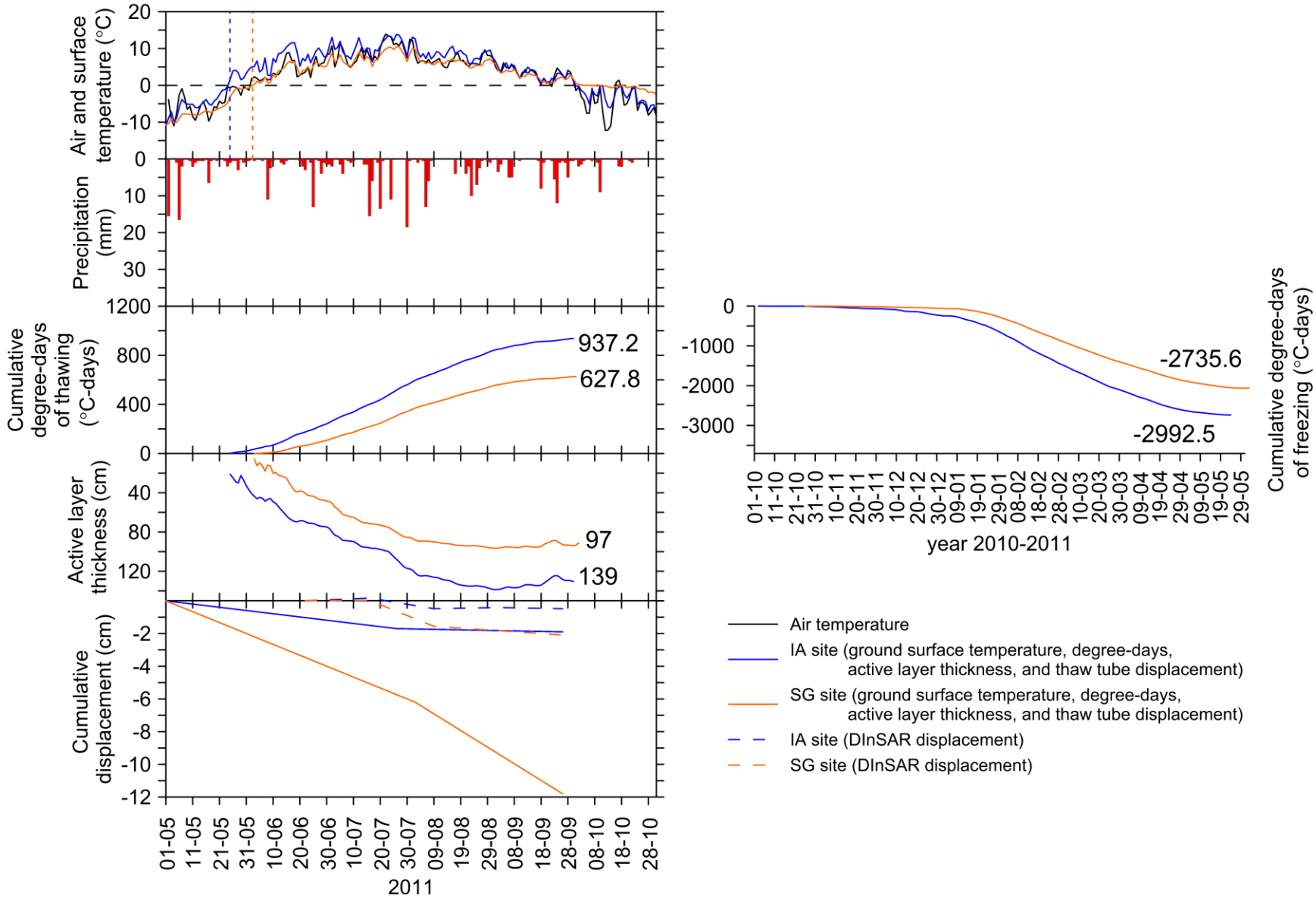

Figure 12: DInSAR time series at two permafrost sites for year 2011 with climatic and soil observations.

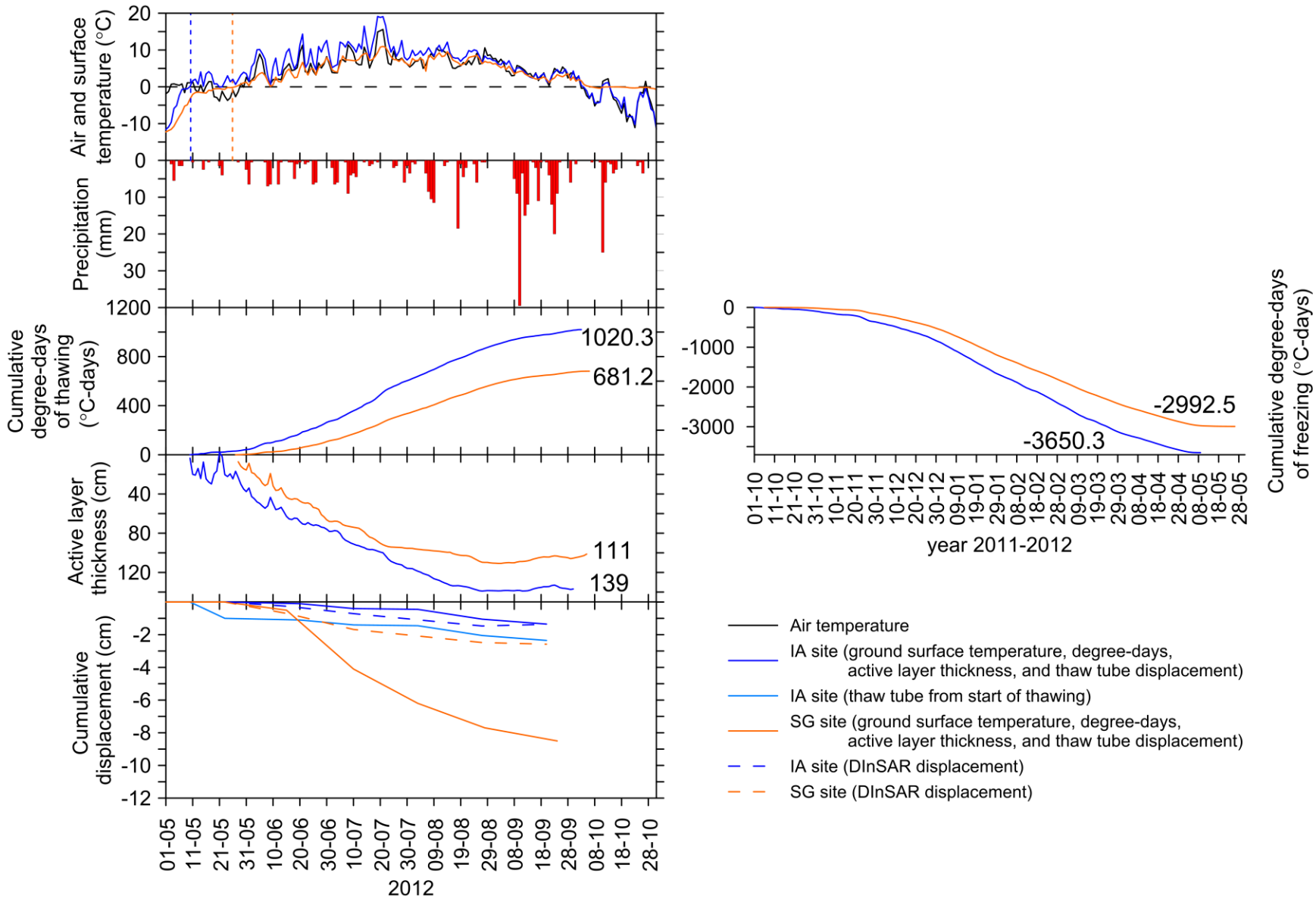

Figure 13: DInSAR time series at two permafrost sites for year 2012 with climatic and soil observations.

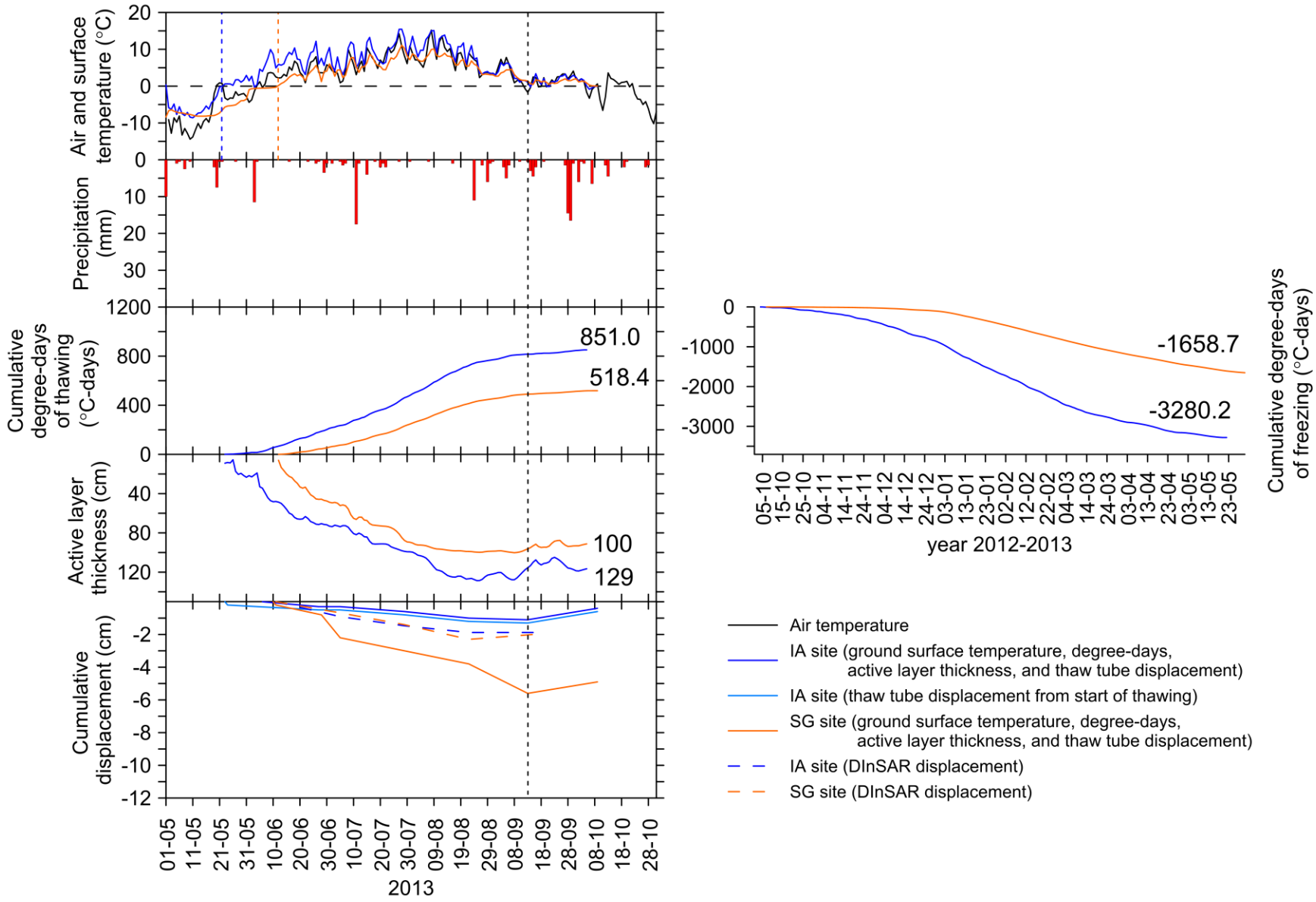

Figure 14: DInSAR time series at two permafrost sites for year 2013 with climatic and soil observations.

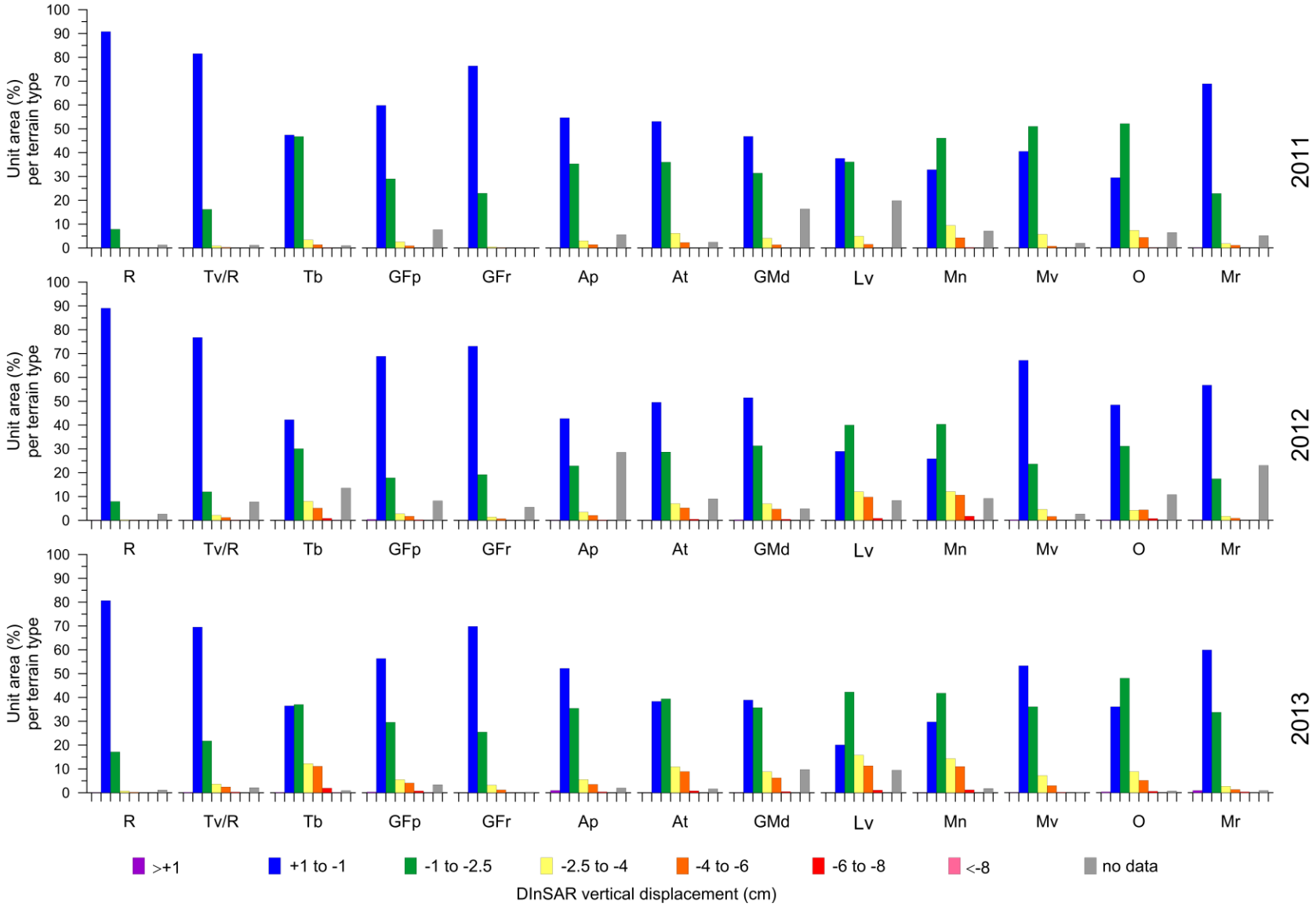

Figure 15: Percentage for each class of DInSAR seasonal surface displacement per surficial geology unit for 2011, 2012 and 2013.

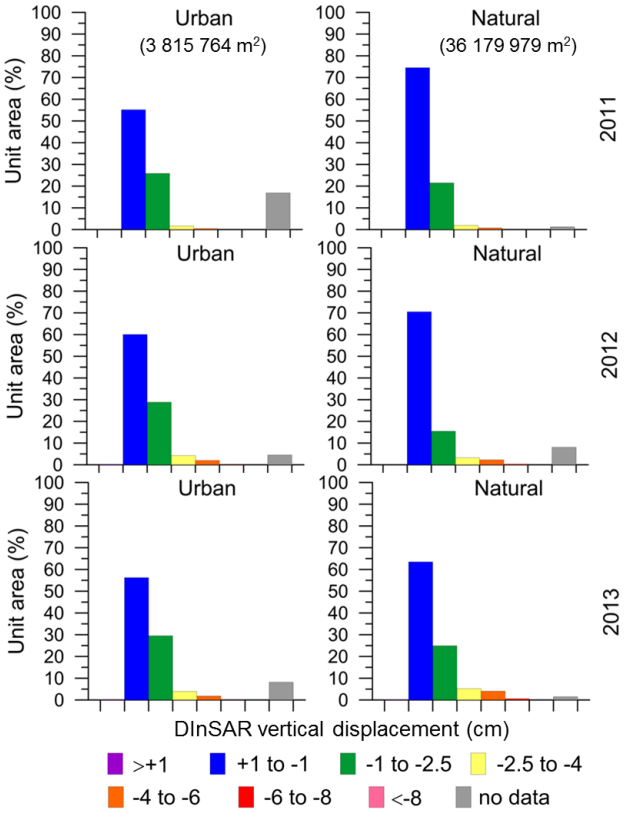

Figure 16: Percentage for each class of DInSAR seasonal surface displacement in urban and natural terrain for 2011, 2012 and 2013.

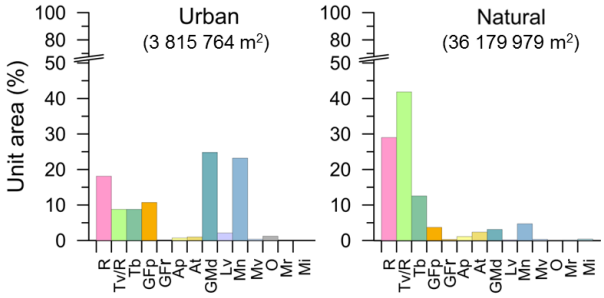

Figure 17: Percentage of each surficial geology unit contained within the urban and natural terrain.

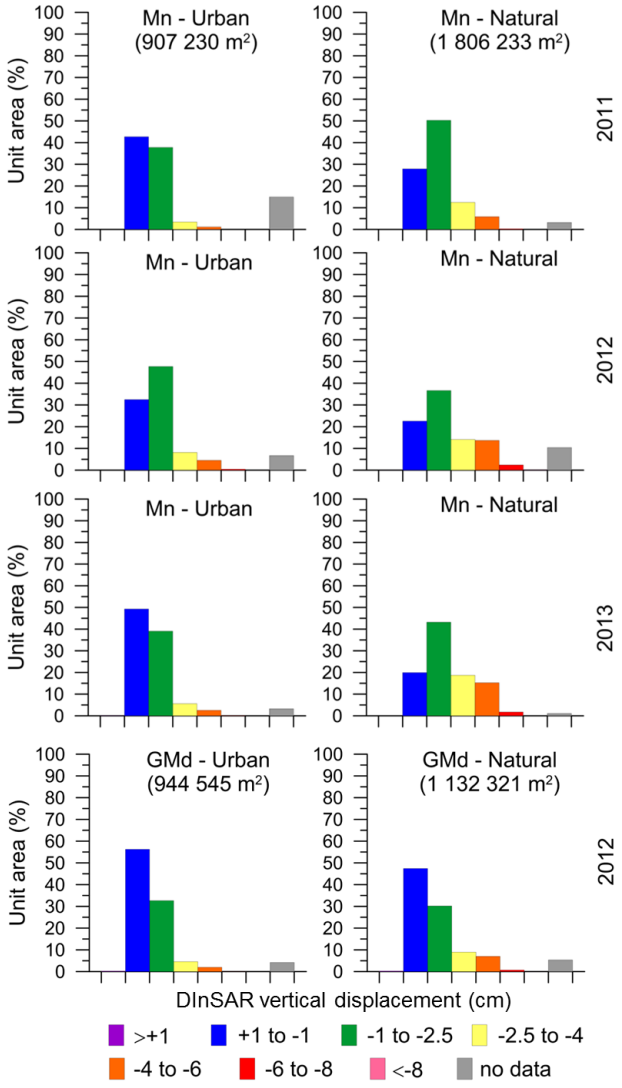

Figure 18: Percentage for each class of DInSAR seasonal surface displacement in urban and natural terrain for surficial units Mn (2011 – 2013) and GMd (2012).

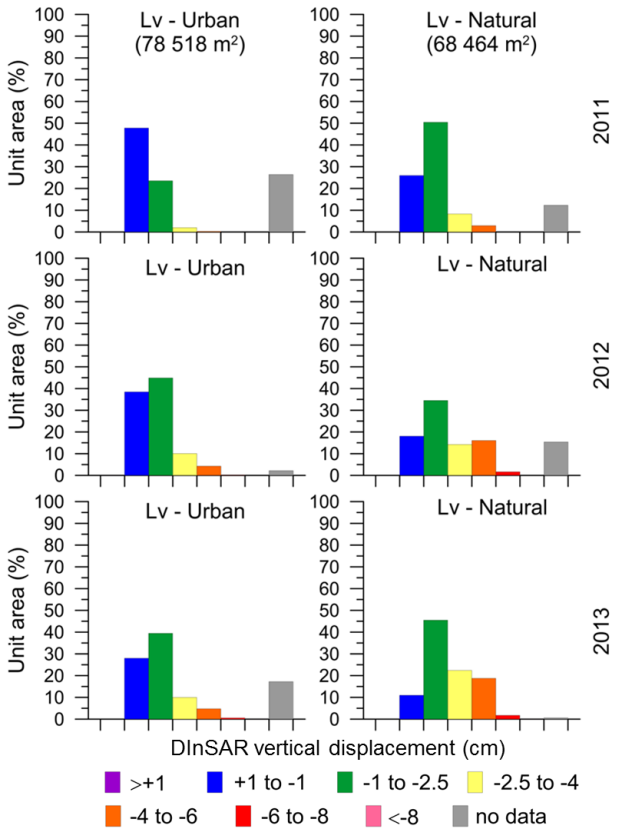

Figure 19: Percentage for each class of DInSAR seasonal surface displacement in urban and natural terrain for surficial unit Lv (2011 – 2013).

Figure 20: Glaciofluvial (GF) boulder fields covered by vegetation. Surface water is present between the boulder field.